6 July 2001

ELSEVIER

Chemical Physics Letters 342 (2001) 148–154

CHEMICAL
PHYSICS
LETTERS

www.elsevier.com/locate/cplett

Monte Carlo simulations of sorption and diffusion of isobutane in silicalite

D. Paschek *, R. Krishna

Department of Chemical Engineering, University of Amsterdam, Nieuwe Achtergracht 166, 1018 WV Amsterdam, The Netherlands

Received 5 February 2001; in final form 20 March 2001

Abstract

We report kinetic Monte Carlo (KMC) and configurational-biased Monte Carlo (CBMC) simulations of isobutane adsorbed in zeolite silicalite. The CBMC simulations provide evidence for the presence of repulsive interactions between molecules adsorbed at adjacent intersection and straight-channel sites. KMC simulations show that even weak repulsive interactions have a strong influence on the diffusivities at higher loadings and therefore could serve as a possible explanation for the experimentally observed change of the apparent activation energy of self- and Maxwell–Stefan diffusion coefficients in this regime. © 2001 Elsevier Science B.V. All rights reserved.

1. Introduction

The proper description of diffusive transport within zeolitic materials is of considerable importance in practice because of the many applications in catalytic reaction and separation processes [1,2]. A variety of models and techniques have been used to describe diffusion within zeolites, ranging from phenomenological models such as the Fick's law of diffusion [1,2] and the Maxwell–Stefan formulation [3,4] to Monte Carlo simulations [5] and Molecular Dynamics (MD) [6] techniques.

Recent experimental work on silicalite-membrane permeation of alkanes [7–9] has shown that the Maxwell–Stefan approach provides a suitable description for quite a number of compounds. However, for the case of isobutane, the membrane-derived Maxwell–Stefan mobilities exhibit a curious deviation from an apparent Arrhenius behavior when the loading exceeds a value of four molecules per unit cell. Moreover, the measured self-diffusivities are about one order of magnitude smaller than the obtained Maxwell–Stefan diffusivities [7].

In order to get some insight into the dynamics of the adsorbed isobutane and to seek some explanation for this curious behavior, we employ configurational-biased Monte Carlo (CBMC) simulations of an atomic detail potential model, as well as kinetic Monte Carlo (KMC) simulations of a coarse-grained representation of the adsorption system.

2. Configurational-biased Monte Carlo simulations

In order to obtain adsorption isotherms and molecule distributions we use CBMC simulations of a realistic model of isobutane in silicalite. The simulations were carried out in the grand

---

* Corresponding author. Fax: +31-20-525-5604.
E-mail address: paschek@its.chem.uva.nl (D. Paschek).

0009-2614/01/$ - see front matter
PII: S0009-2614(01)00382-7

canonical ensemble, where the chemical potential for the adsorbed phase and the temperature are fixed. For all CBMC simulations the BIGMAC simulation code [10] has been employed. In order to ensure chemical equilibrium, it is essential to successfully exchange particles with the reservoir. In the present simulations, a flexible alkane is grown atom by atom in such a way that the ‘empty spaces’ in the zeolite are found. The bias of the growing scheme is exactly removed by a modification of the acceptance rules [11]. A more detailed description of the CBMC method can be found in [12]. The interaction potential employed here has been recently proposed by Vlugt et al. [11] and assumes the zeolite to be rigid. Moreover, the CH_n-groups are treated as ‘united atoms’, which are represented by a single Lennard–Jones interaction site. Our simulation box consists of 16 $(2 \times 2 \times 4)$ unit cells of silicalite. The results shown here refer to simulations that consisted typically of 3×10^5 simulation cycles, where the last 10^5 steps were used for analyzing purposes.

Branched alkanes, such as isobutane, show an adsorption isotherm with an inflection. Recent CBMC simulation by Vlugt et al. [11] have demonstrated, that it is likely that the presence of an inflection is related to the siting of molecules in the silicalite interior. The channel space can be subdivided into straight channels, zig-zag channels and the intersections connecting them. Branched components, like isobutane, prefer to be located at the more spacious intersections. The effect of sites with different adsorption strengths is also of importance for the form of the adsorption isobars (100 and 170 kPa) as shown in Fig. 1a. Here, the CBMC simulation data, that were derived from a series of CBMC isotherms, are compared with the experimental data of Millot et al. [7]. The CBMC simulation data were fitted to a dual site Langmuir isotherm

$$\Theta = \Theta_A \frac{b_A p}{1 + b_A p} + \Theta_B \frac{b_B p}{1 + b_B p}, \tag{1}$$

where p is the partial pressure of isobutane and b_A and b_B are the Langmuir constants for intersections (A) and channel sites (B) with $b_A(T) = 8.28 \times 10^{-11}\ \mathrm{Pa}^{-1} \times \exp(-48.5\ \mathrm{kJ\ mol}^{-1}/\mathrm{RT})$ and $b_B(T) = 1.27 \times 10^{-13}\ \mathrm{Pa}^{-1} \times \exp(-43.0\ \mathrm{kJ\ mol}^{-1}/\mathrm{RT})$. Θ_A and Θ_B are the corresponding saturation loadings with $\Theta_A = 4$ and $\Theta_B = 6$ molecules per

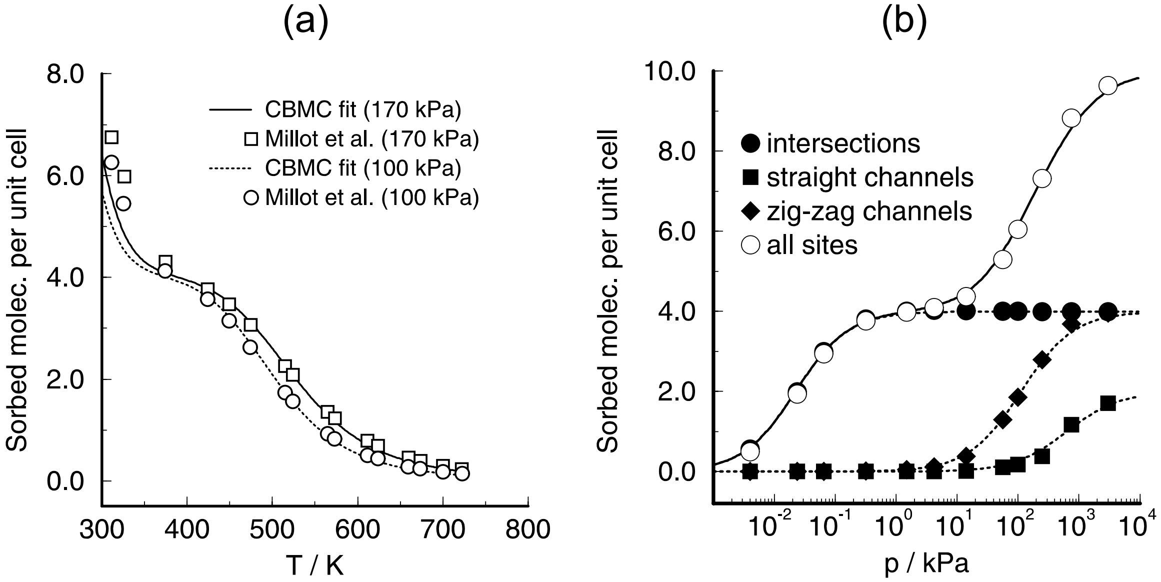

Fig. 1. (a) Adsorption isobars of isobutane in silicalite obtained for 100 and 170 kPa. The open symbols refer to the experimental data of Millot et al. [7] while the lines represent data fitted to a series of CBMC simulations. (b) Adsorption isotherms (obtained from CBMC simulations) of isobutane in silicalite at $T = 300$ K for the different parts of the silicalite interior.

unit cell. The near quantitative agreement between simulated and experimental data might justify a more detailed analysis of the molecular distribution in terms of the simulated isobutane isotherm at 300 K outlined in Fig. 1b. Details on how the siting has been determined can be found in [13]. The four intersection sites per unit cell are already filled at rather low pressures. With increasing pressure, also the channel sites are getting occupied. Note, that the Van der Waals radius of the adsorbed isobutane plays an important role for the siting, as can be guessed from Fig. 2. In Fig. 2 a snapshot of isobutane in the silicalite interior at a pressure of 3000 kPa is shown. This represents a region where the saturation loading is almost reached. Since the zig-zag channels are long enough ($\approx$1.2 nm), there is almost no interference with the molecules adsorbed at the intersection sites. Consequently, all four zig-zag sites get occupied and the position of the molecules in the zig-zag channels stay almost unperturbed even at very high pressures. The straight channels ($\approx$1.0 nm), however, are slightly shorter. Therefore the molecules adsorbed at the intersections and within the zig-zag channels feel a significant repulsive interaction. As can be seen in Fig. 2, the molecules adsorbed at intersections relax laterally in y-direction (along the straight channels) if a molecule is adsorbed at an adjacent straight channel position. A close examination of Fig. 2 reveals that almost every second straight channel site is left empty, since it is blocked by the neighboring (laterally relaxing) intersection site molecules. As a consequence, the loading capacity of the straight channels is significantly reduced from 4 to about 2 molecules per unit cell.

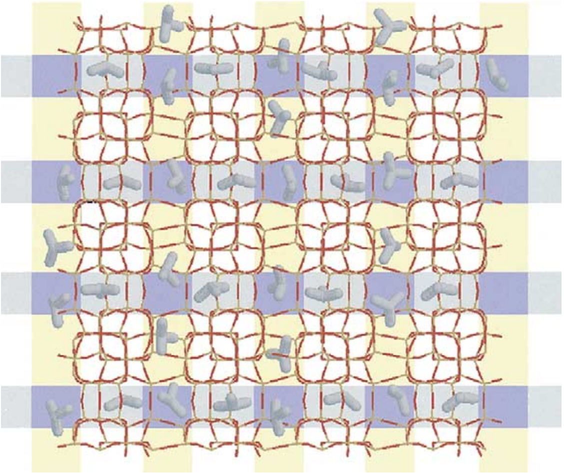

Fig. 2. Snapshot showing the location of isobutane at 300 K and 3000 kPa. The view-axis is in z-direction (compare with Fig. 3). The different parts of the silicalite interior are highlighted by a different color. Zig-zag channels are indicated grey, straight channels are yellow and intersections are blue.

All in all, due to molecule–molecule repulsion of molecules adsorbed at intersections and straight channels, the total saturation capacity is limited to about 10 molecules per unit cell. The impact of repulsive interactions on the mobility of the adsorbed phase is discussed in the Section 3.

3. Kinetic Monte Carlo simulations

We perform KMC simulations of a system of adsorbed particles on discrete lattice sites with nearest neighbor interactions. Particles can move from one site to a neighboring site via hops. The probability per unit time to move from one site to another is determined by transition rates, which have been chosen to reproduce published experimental and simulated (MD simulation) data [7,14]. A standard KMC methodology is employed to propagate the system (see [5,15–17]). A hop is made every KMC step and the system clock is updated with variable time steps. For a given configuration of random walkers on the silicalite lattice, a process list containing all possible M moves to vacant sites is created. Each possible move i is associated with a transition probability k_i. Note, that these values depend on the particular type of move a particle attempts (such as moves along the straight channels or the zig-zag-channels) as well as on the possible occupation of neighboring sites. The *mean* elapsed time τ is the inverse of the *total* rate coefficient

$$\tau^{-1} = k_{\text{total}} = \sum_{i=1}^{M} k_i, \tag{2}$$

which is determined as sum over all processes contained in the process list. The actual KMC time step Δt for a given configuration is randomly chosen from a Poisson distribution

$$\Delta t = -\ln(u)k_{\text{total}}^{-1}, \tag{3}$$

where $u \in [0, 1]$ is a uniform random deviate. The timestep Δt is independent from the chosen hopping process. To select the actual jump, we define process probabilities according to $P_i = \sum_{j=1}^{i} k_j/k_{\text{total}}$. The ith process is chosen, if $P_{i-1} < v \leqslant P_i$, where $v \in [0, 1]$ is another uniform random deviate. After having performed a hop, the process list is updated. In order to avoid wall effects we employ periodic boundary conditions. In keeping with our previous findings [5], the finite size-effect on diffusivity was found to be negligible at a size of $5 \times 5 \times 5$ unit cells. About 10^7 simulation steps were performed for each simulation. The runlength depends strongly on the number of possible jump processes, but even the most time-consuming simulations could be completed within a few hours on a single IBM SP2-node.

According to results concerning the localization of the adsorbed isobutane molecules, we propose a discretization of the zeolite channel structure using 12 sites per unit cell, as shown in Fig. 3. The transition probabilities (per unit time) to attempt a hop from an intersection site (*in*) to any other neighboring site (*st*: straight channel, *zz*: zig-zag channel) is defined by

$$\begin{aligned} k_{\text{in}\to\text{st}}(T) &= k_\infty \exp(-E_a/\text{RT}), \\ k_{\text{in}\to\text{zz}}(T) &= k_{\text{in}\to\text{st}}(T)/3, \end{aligned} \tag{4}$$

where k_∞ is the so-called frequency factor, which characterizes individual particle mobilities at infinitely high temperature. E_a represents the activation energy for the assumed Arrhenius behavior of the hopping processes. The ratio of 3 between the different hopping rates is motivated by recent MD simulations [14,18] which reveal ratios between 2 and 3 for the mobilities in *x*- and *y*- directions for several alkanes. In order to match the experimental Maxwell–Stefan diffusivity data of Millot et al. [7], values for $k_\infty = 8.0 \times 10^{12}\ \text{s}^{-1}$ and $E_a = 1.3$ kJ mol^{-1} were employed. To account correctly for the particle distributions according to the experimental adsorption isotherms, the transition probabilities for the reversed moves have to be modified by a factor

$$\begin{aligned} k_{\text{st}\to\text{in}}(T) &= k_{\text{in}\to\text{st}}(T)b_{\text{B}}(T)/b_{\text{A}}(T), \\ k_{\text{zz}\to\text{in}}(T) &= k_{\text{in}\to\text{zz}}(T)b_{\text{B}}(T)/b_{\text{A}}(T), \end{aligned} \tag{5}$$

where $b_{\text{A}}(T)$ and $b_{\text{B}}(T)$ are the experimentally determined Langmuir constants for the adsorption at intersections (A) with $b_{\text{A}}(T) = 8.97 \times 10^{-11}\ \text{Pa}^{-1} \times \exp(-50.2\ \text{kJ mol}^{-1}/\text{RT})$ and channel sites (B) with $b_{\text{B}}(T) = 1.15 \times 10^{-13}\ \text{Pa}^{-1} \times \exp(-44.9\ \text{kJ mol}^{-1}/\text{RT})$ according to [19]. In order to account

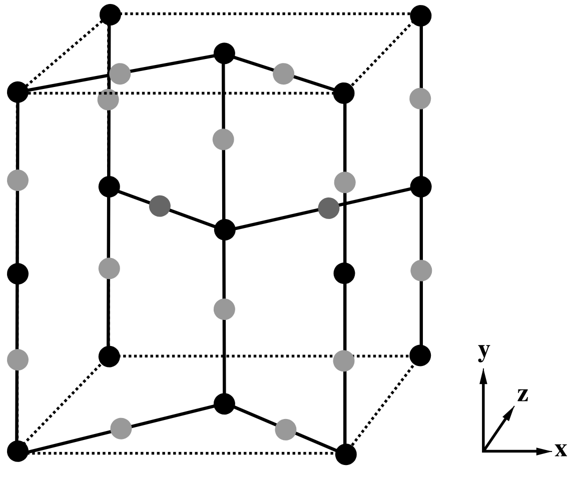

Fig. 3. Diffusion unit cell used for KMC simulations. Intersection (*in*) sites are connected via straight channel (*st*) sites and zig-zag (*zz*) channel sites. Unit cell parameters: $a = 2.01$ nm (x), $b = 1.99$ nm (y), and $c = 1.34$ nm (z).

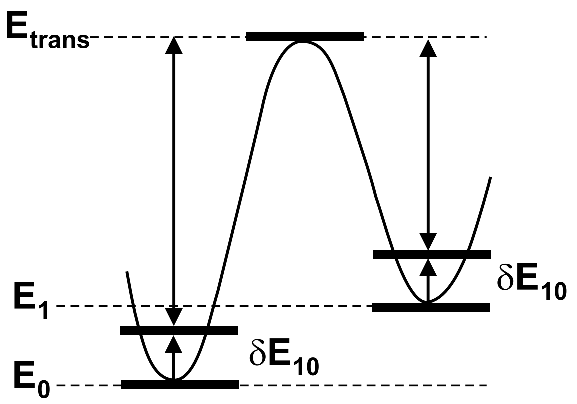

Fig. 4. Energy scheme employed in the KMC simulations used here. Two particles adsorbed at adjacent sites are feeling a repulsive interaction δE_{10}. The scheme is explained in the text.

for nearest neighbor interactions, the transition rates have to be changed if another particle occupies an adjacent site. The employed procedure is illustrated in Fig. 4. It is based on the assumption that the logarithm of rate of any process is proportional to the height of the energy barrier, as for example given by $E_{\mathrm{trans}} - E_0$ for the move '0 → 1'. Consider now two neighboring particles at positions '0' and '1': In order to ensure energy conservation, both particles have to feel the same repulsive interaction δE_{10}. The depth of the potential well of a particle at a position α (e.g., at position '0') is modified by δE_α, which is determined by summing over all possible nearest neighbor interactions

$$\delta E_\alpha = \sum_\beta \delta E_{\alpha\beta}. \tag{6}$$

Here, β indicates all occupied nearest neighbor positions with respect to α. In the KMC scheme, the rates for all possible moves of the particle located at α have to be changed by a factor

$$k'_{\alpha\to\beta'} = k_{\alpha\to\beta'} \exp(\delta E_\alpha/\mathrm{RT}). \tag{7}$$

Here, β' denotes all empty nearest neighbor positions with respect to α. Since only nearest neighbor interactions are involved, the scheme is simple and the computional effort moderate. According to our CBMC findings, we have introduced repulsive interactions only between particles adsorbed at intersection sites and straight-channel sites. From the KMC simulations we calculate *jump* diffusivities D_{jump}, which have been shown to represent the so-called 'corrected diffusivities' (as shown by the work of Reed et al. [15], as well as Uebing et al. [20,21]) and therefore correspond to experimental Maxwell–Stefan diffusivities. In addition, we calculate *self* diffusivities D_{self}, which correspond to tracer experiments like PFG-NMR or QENS. Here

$$D_{\mathrm{jump}} = \frac{1}{6} \lim_{\Delta t\to\infty} \frac{1}{\Delta t} \left\langle \left(\frac{1}{N} \sum_{i=1}^{N} \vec{r}_i(t+\Delta t) - \vec{r}_i(t) \right)^2 \right\rangle \tag{8}$$

denotes the mean square displacement of the center of gravity of all N adsorbed particles and

$$D_{\mathrm{self}} = \frac{1}{6} \lim_{\Delta t\to\infty} \frac{1}{\Delta t} \frac{1}{N} \sum_{i=1}^{N} \left\langle \left(\vec{r}_i(t+\Delta t) - \vec{r}_i(t) \right)^2 \right\rangle \tag{9}$$

represents the mean square displacement of the individual particles.

The Maxwell–Stefan diffusivities for isobutane in silicalite are shown in Figs. 5a,b. In both diagrams the large open symbols represent Maxwell–Stefan data that was recalculated by using the original flux data of [7], applying the Maxwell–Stefan theory that has been explicitly adapted to the particlar problem (see [22]). Considered were both reported experiments with pressure drops of 50 and 70 kPa across the silicalite membrane [7]. The experimental data reveals a sharp change in the apparent activation energy at a temperature of about 400–420 K. This is just the range where the molecular loading exhibits a value of about four molecules per unit cell (see Fig. 1a). A possible explanation for this behavior is provided by the KMC simulations discussed below.

In Fig. 5a the simulated jump diffusivities are compared with the experimental Maxwell–Stefan diffusivities. The loading of the lattice model corresponds to the 170 kPa isobar and was determined by using the Langmuir parameters of [19] which are given above. The influence of the nearest neighbor repulsion $\delta E_{\alpha\beta}$ is systematically varied. First of all we have to denote that the apparent activation energy in the KMC model is to a large extent determined by the reduced particle mobilities, which is simply a consequence of the decreasing number of degrees of freedom at increased loading. This 'site-blocking' effect is strongly modulating the diffusivity curve. Even with nearest neighbor interactions fully absent ($\delta E_{\alpha\beta} = 0.0$) this curve reveals already a minimum at about 400 K. Introducing a repulsive interaction now does not affect the diffusivity at higher temperatures than 420 K significantly, since the particles are mostly located at intersection sites and therefore hardly interact. At lower temperatures, however, some particles are forced to occupy straight channel sites and therefore have to be 'in contact' with molecules located at the intersections. As a consequence, the particle–particle

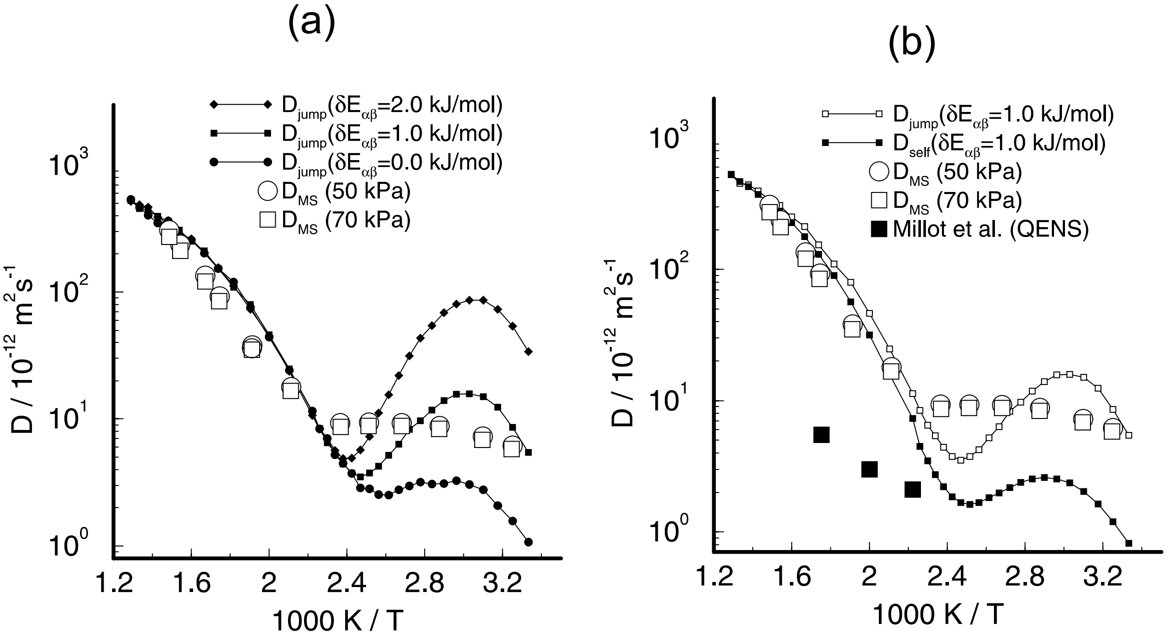

Fig. 5. Diffusion coefficients for isobutane adsorbed in silicalite: (a) Large symbols: experimentally determined Maxwell–Stefan diffusion coefficients. Small symbols: jump diffusion coefficients obtained from KMC simulations for different particle–particle interaction strengths $\delta E_{\alpha\beta}$. (b) Large open symbols: experimentally determined Maxwell–Stefan diffusion coefficients. Large closed squares: experimentally determined self diffusion coefficients (QENS). Small symbols: diffusion coefficients obtained from KMC simulations (small open squares: jump diffusion coefficients; small closed squares: self diffusion coefficients). The experimental data is according to [7].

repulsion results in an increasing mobility. A value of about $\delta E_{\alpha\beta} = 1.0$ kJ/mol gives best coincidence with the reported experimental data. However, we have to state that the coincidence is not fully satisfying, especially in the ‘loop region’ below 400 K. The reason for this maybe twofold: one aspect might be related with the definition of sharp discrete lattice sites in the KMC model. In a real system the molecules interact smoothly and have the opportunity to relax laterally and will avoid strong repulsive interactions by rearranging orientationally and conformationally. The possible relaxation of the zeolite lattice might also play a role here. So, it is likely that these effects could wash out the sharp extrema provided by the lattice model. Another point is related to a deficiency of the KMC lattice model. At full loading the mobility of the particles in the KMC-model will go to zero due to the absence of any further motional degrees of freedom. However, this scenario is quite unrealistic, since in this region mobility could still persist due to the presence of collective motions. Therefore, it might be possible that the KMC-model overestimates the loading dependence of the particle mobility due to the effect of ‘site-blocking’.

In Fig. 5b the simulated jump and self diffusion coefficients are compared with the experimental data determined from membrane permeation and QENS experiments. The reported QENS tracer diffusivities are about one order of magnitude smaller than the membrane derived Maxwell–Stefan values. Please note, that also the KMC simulations reveal self diffusion coefficients that are significantly smaller than the obtained jump diffusivities. However, in contrast to the experimental observations, a difference of one order of magnitude is reached only at the very smallest temperatures considered. In the temperature range where the experimental data were conducted, the self diffusivities are only slightly smaller than the jump diffusivities. So, the KMC simulations cannot provide clues for the apparent discrepancy between QENS and Maxwell–Stefan data.

4. Conclusions

CBMC simulations reveal evidence for the presence of repulsive intermolecular interactions between molecules adsorbed at intersections and adjacent straight channel sites. These repulsive interactions are a simple geometrical consequence of the size of the adsorbed molecules and size of the zeolite structure. KMC simulations of a coarse-grained model system with particles adsorbed at discrete lattice sites reveal a change of the apparent activation energy of the calculated Maxwell–Stefan diffusion coefficients, which has some similarity to the behavior of the experimentally determined Maxwell–Stefan diffusivities. Repulsive interactions between molecules adsorbed at intersection sites and straight channel sites enhance the mobility particularly at lower temperatures. Here, even small repulsive interaction energies have a huge effect. Finally, a comparison of jump and self diffusivities determined from KMC simulations does not provide clues for the apparent discrepancy between experimental QENS and Maxwell–Stefan diffusivity data.

Acknowledgements

D.P. and R.K. acknowledge a generous grant ‘Programmasubsidie’ from the Netherlands Organisation for Scientific Research (NWO). The Gesellschaft für Mathematik und Datenverarbeitung (GMD) in Bonn, Sankt Augustin, Germany, is acknowledged for providing computer time.

References

[1] J. Kärger, D.M. Ruthven, Diffusion in Zeolites and other Microporous Solids, Wiley, New York, 1992.

[2] D.M. Ruthven, S. Farooq, K.S. Knaebel, Pressure Swing Adsorption, VCH Publishers, New York, 1994.

[3] R. Krishna, J.A. Wesselingh, Chem. Eng. Sci. 52 (1997) 861.

[4] F. Kapteijn, J.A. Moulijn, R. Krishna, Chem. Eng. Sci. 55 (2000) 2923.

[5] D. Paschek, R. Krishna, Phys. Chem. Chem. Phys. 2 (2000) 2389.

[6] R. Haberlandt, S. Fritzsche, G. Peinel, K. Heinzinger, Molecular Dynamics, Vieweg, Braunschweig, 1995.

[7] B. Millot, A. Methivier, H. Jobic, H. Moueddeb, M. Bee, J. Phys. Chem. B 103 (1999) 1096.

[8] B. Millot, A. Methivier, H. Jobic, I. Clemencon, B. Rebours, Langmuir 15 (1999) 2534.

[9] B. Millot, A. Methivier, H. Jobic, H. Moueddeb, J.A. Dalmon, Microporous Mesoporous Mater. 38 (2000) 85.

[10] The BIGMAC simulation program is authored by T.J.H. Vlugt, B. Smit, Information is available on the web: http://molsim.chem.uva.nl/bigmac.

[11] T.J.H. Vlugt, R. Krishna, B. Smit, J. Phys. Chem. B 103 (1999) 1102.

[12] T.J.H. Vlugt, M.G. Martin, B. Smit, J.I. Siepmann, R. Krishna, Mol. Phys. 94 (1998) 727.

[13] R. Krishna, D. Paschek, Phys. Chem. Chem. Phys. 3 (2001) 453.

[14] A. Bouyermaouen, A. Bellemans, J. Chem. Phys. 108 (1997) 2170.

[15] D.A. Reed, G. Ehrlich, Surf. Sci. 105 (1981) 603.

[16] K.A. Fichthorn, W.H. Weinberg, J. Chem. Phys. 95 (1991) 1090.

[17] C. Saravanan, S.M. Auerbach, J. Chem. Phys. 107 (1997) 8132.

[18] E.B. Webb III, G.S. Grest, M. Mondello, J. Phys. Chem. B 103 (1999) 4949.

[19] B. Millot, A. Methivier, H. Jobic, Fundamentals of Adsorption, in: F. Meunier (Ed.), vol. 6, Elsevier, Paris, 1998, p. 273.

[20] C. Uebing, V. Pereyra, G. Zgrablich, Surf. Sci. 366 (1996) 185.

[21] A.A. Tarasenko, L. Jastrabik, C. Uebing, Langmuir 15 (1999) 5883.

[22] R. Krishna, T.J.H. Vlugt, B. Smit, Chem. Eng. Sci. 54 (1999) 1751.